POSITRON ANNIHILATION ANGULAR CORRELATION MEASUREMENTS IN NEUTRON-IRRADIATED NIOBIUM AND NIOBIUM-3WT%ZIRCONIUM

Kuramoto, Eiichi
Research Institute for Applied Mechanics, Kyushu University : Associate Professor

Kitajima, Kazunori
Research Institute for Applied Mechanics, Kyushu Uniuersity : Professor

Hasegawa, Masayuki
The Oarai Branch, The Research Institute for Iron, Steel and Other Metals, Tohoku University : Research Associate

https://doi.org/10.5109/6617892

出版情報：Reports of Research Institute for Applied Mechanics. 26 (81), pp.1-21, 1978-07. 九州大学応用力学研究所
バージョン：
権利関係：

Reports of Research Institute for Applied Mechanics
Vol. XXVI, No. 81, 1978

POSITRON ANNIHILATION ANGULAR CORRELATION MEASUREMENTS IN NEUTRON-IRRADIATED NIOBIUM AND NIOBIUM-3WT%ZIRCONIUM

By Eiichi KURAMOTO*, Kazunori KITAJIMA**
and Masayuki HASEGAWA***

Positron annihilation angular correlation measurements have been performed in niobium and niobium-3wt%zirconium irradiated by neutron to a total dose of 5×10^{20}n/cm^2 at about 300°C. Full width at half maximum of the angular correlation curve was decreased by irradiation in both cases. Reduction percentages were 25% and 20% in niobium and niobium-3wt%-zirconium, respectively, and recovered to the original value after annealing at 1100°C in niobium. It cannot be considered as realistic that single vacancies or dislocation loops induced by irradiation cause such large reductions in width. Hence it should be considered that microvoids or depleted zones are formed during irradiation, probably, both of them in niobium and depleted zones only in niobium-3wt%zirconium. This conclusion was supported by the annealing behavior of yield strength in niobium.

1. Introduction

Recently positron annihilation measurements have become an important technique in the studies of lattice defects in crystals. As for the irradiation damage in metals, annihilation behavior of positrons in vacancy clusters (or depleted zones) and voids must be quite different from that in the perfect matrix. A large number of investigations, especially about voids, have so far been performed in various metals, e.g., molybdenum[1-7], aluminum[8-10] and nickel[11,12]. From standpoints of both of experiments[13] and theoretical considerations[14,15], it has been established that positrons in microvoids give longer lifetime and narrower width of an angular correlation curve with increasing the microvoid size. In this paper will be reported the results of angular correlation measurements on neutron-irradiated niobium and niobium-

* Associate Professor, Research Institute for Applied Mechanics, Kyushu University.
** Professor, Research Institute for Applied Mechanics, Kyushu Uniuersity.
*** Research Associate, The Oarai Branch, The Research Institute for Iron, Steel and Other Metals, Tohoku University, Oarai, Ibaraki 311-13, JAPAN

3wt%zirconium. In the former microvoid formation can be expected.

2. Experimental Procedures

2.1 Positron Annihilation Angular Correlation Measurements

Positrons used for the study of defects penetrate into the metal with high energy around 1 MeV, but are rapidly slowed down by the interaction with conduction electrons and, at not too low temperatures, are thermalized in times small compared with the lifetime of the positrons. The life of a positron is terminated by annihilation with an electron, the total mass of the pair being converted into electromagnetic radiation. In metals the main contribution to the annihilation rate comes from the conduction electrons and minor contribution comes from the core electrons. The behaviour of positrons in metals must be studied through the γ irradiation emitted during the annihilation process (usually two γ rays in opposite directions). If both members of an annihilating electron-positron pair are at rest, the conservation of energy and linear momentum demands that in two-photon annihilation the two γ rays are emitted with exactly the same energy ($E_\gamma = m_0c^2$ where m_0 is the electron or positron rest mass) and in exactly opposite directions with linear monenta $P_\gamma = \pm m_0c$. If the annihilating pair has a nonvanishing

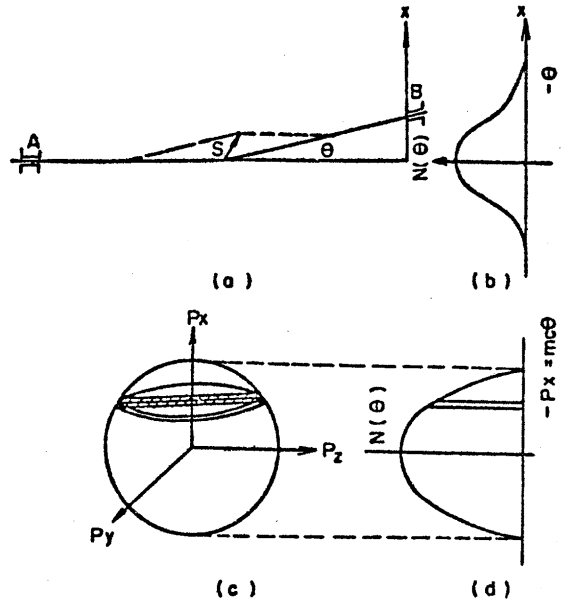

Fig. 1 (a) Principle of positron annihilation, (b) Coincidence counting rates vs angle θ, (c) Electron distribution in momentum space for free electrons, and (d) γ-γ angular correlation for free electrons.

linear momentum p, this symmetry is lost, and the directions of the γ rays differ from 180° by a small angle θ=p/mc. Measurements of the angular correlation of the directions of the photons resulting from a 2γ annihilation give thus information on the linear momentum and hence on the velocity of the annihilating pair. This is illustated in (a) and (b) in Fig. 1. If Fermi surface is a perfect sphere, namely, constructed by free electrons only, the measured angular correlation curve is a parabola, because each value on the angular correlation curve corresponds to the volume of the sliced part of the sphere as shown in (c) and (d) in Fig. 1. Hence the tail of the angular correlation curve comes from the contribution of core electrons. Usually this contribution is approximated by a Gaussian distribution curve.

The schematic diagram of the measuring circuit of the angular correlation is shown in Fig. 2. NaI(Tl) detector is used to count the annihilation quanta. One detector is fixed and the other is located on the moving arm. The distance between two detectors is 4 m. The moving direction of the detector is from down to up. This system has a conventional long slit just

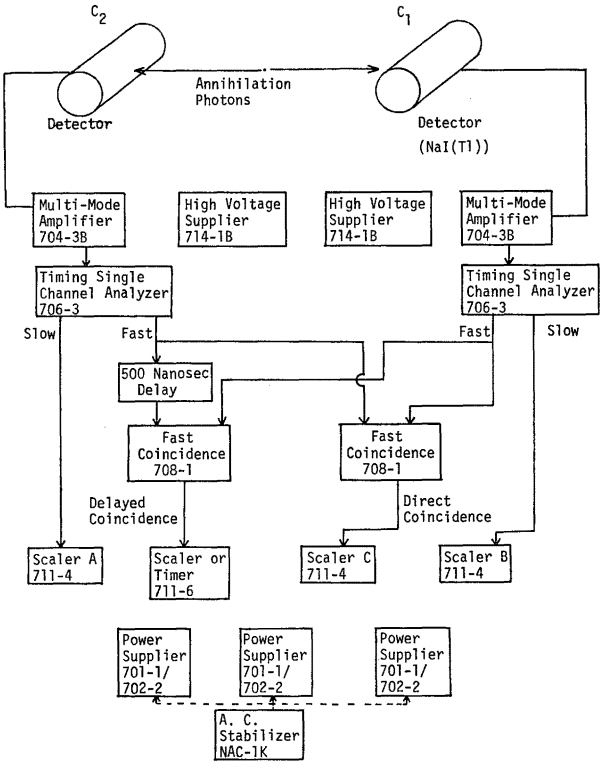

Fig. 2 Schematic diagram of the electronic circuit for the angular correlation measurement.

before the each detector having geometrical resolution of 0.63 mrad (FWHM), details of which were published in the previous paper[16]. As a positron source ^{64}Cu produced by neutron irradiation in JMTR (Hydro-Rabbit irradiation) was used. The counting rate was calculated by the following expression; $P=(N_c-n_c)/(N_a-n_a)$, $n_c=2\tau N_a N_b$, where N_c is the coincidence count, N_a and N_b are single counts for a moving and a fixed counter, respectively, n_c is the chance coincidence count and τ is the resolution time (~25 nsec), n_a is the back ground count for a moving counter.

2.2 Sample Preparation and Neutron Irradiation

High purity niobium of MRC (MARZ-grade) was electron beam zone-melted in vacuum ($\sim 1\times10^{-6}$mmHg) (together with a calculated amount of zirconium sandwiched by two niobium rods (up and down), when the alloy was obtained) and then rolled into a thin sheet of 0.1 mm, which was annealed by direct current heating in ultra high vacuum ($\sim 5\times10^{-9}$ mmHg) for one hour at about 2000°C. Specimens thus obtained were polycrystals of coarse grain (~2 mm). The specimens were irradiated in the H-7-3 hole of the JMTR reactor at about 300°C to a total dose of 4.8×10^{20} n/cm^2 (> 1MeV) and were preserved in the hot-cell for 8 months before use for positron annihilation measurements in order to reduce the back ground due to the induced activity of the specimens. Two specimens of a size 10 mm×10 mm×0.1 mm were piled up on the specimen holder for one test run to obtain an enough thickness (0.2 mm) for stopping positrons in the specimen.

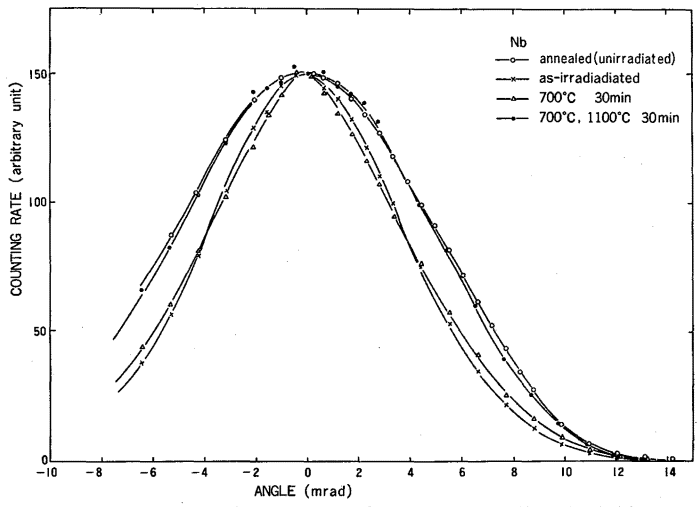

Fig. 3 Angular correlation curves of neutron-irradiated niobium; (open circle) unirradiated specimen, (cross) neutron-irradiated with 4.8×10^{20} n/cm^2, (triangular) annealed at 700°C for 30 min, (solid circle) annealed at 700°C and 1,100°C for 30 min.

3. Experimental Results

Figure 3 shows the angular correlation curves of niobium specimens unirradiated, as-irradiated, annealed at 700°C (30 min, 2×10^{-5} mmHg) 1100

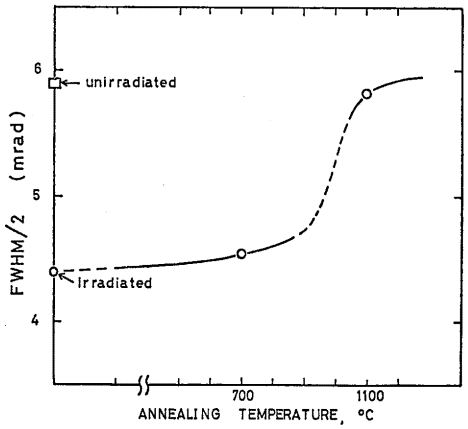

Fig. 4 Effects of the isochronal annealing for 30 min on the full width at half maximum (FWHM) of the angular correlation curve of niobium irradiated by neutron. The same crystal was used for each annealing.

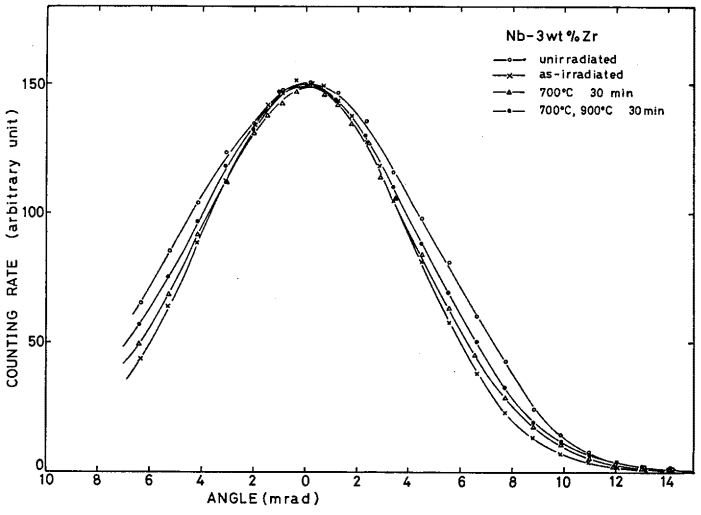

Fig. 5 Angular correlation curves of neutron-irradiated niobiobium-3wt% zirconium; (open circle) unirradiated specimen, (cross) neutron-irradiated with 4.8×10^{20} n/cm^2, (triangular) annealed at 700°C for 30 min, (solid circle) annealed at 700°C and 900°C for 30 min.

°C for 30 min. The full width at half maximum (FWHM) of as-irradiated specimen is in 25% reduction compared with that of unirradiated specimen and recovered completely by annealing up to 1100°C as shown in Fig. 4. Annealing at 700°C did not give any recovery to FWHM but a slight change to the shape of an angular correlation curve as seen in Fig. 3. Figure 5 shows the angular correlation curves of niobium-3wt%zirconium specimens unirradiated, as irradiated, annealed at 700°C and 900°C. FWHM of as-irradiated specimen is in 20% reduction compared with that of unirradiated one. In niobium-3wt%zirconium recovery already started at 700°C annealing and at 900°C almost half of the reduction was recovered as shown in Fig. 6.

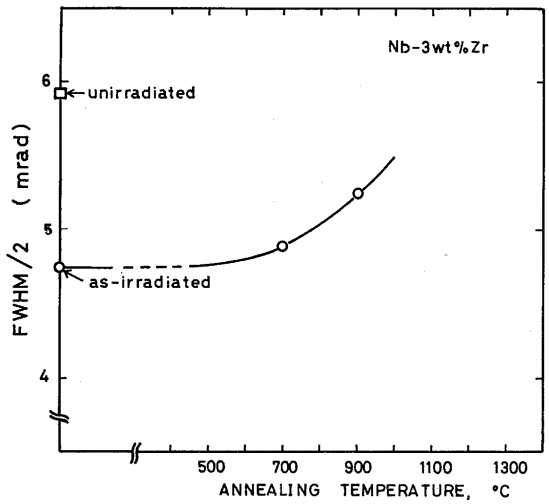

Fig. 6 Effects of the isochronal annealing for 30 min on FWHM of the angular correlation curve of niobium-3wt% zirconium irradiated by neutron. The same specimen was used for each annealing.

Isochronal annealing experiments of the yield strength was also performed for niobium using specimens of the shape of 8 mm×30 mm×0.1 mm neutron-irradiated under almost same condition (7.2×10^{20} n/cm^2, ~300°C). Recovery of the yield strength due to isochronal annealing (20 min, $\sim2\times10^{-5}$ mmHg) is shown in Fig. 7. Tensile tests were performed at room temperature using two specimens, namely, one specimen was tested repeatedly after annealing at 500°C, 700°C, 900°C successively and the other one at 600°C, 800°C, 1000°C in order to avoid the work hardening caused by repeated tests of the same specimen. It is clearly seen that recovery occurs in two steps, i.e., around 750°C aad 1000°C. A small increase of the yield stess is seen between as-irradiated and 500°C annealed specimen, which might be some radiation-anneal hardening. On the other hand, niobium specimen of 1mmϕ×30 mm irradiated by neutron to a lower dose of

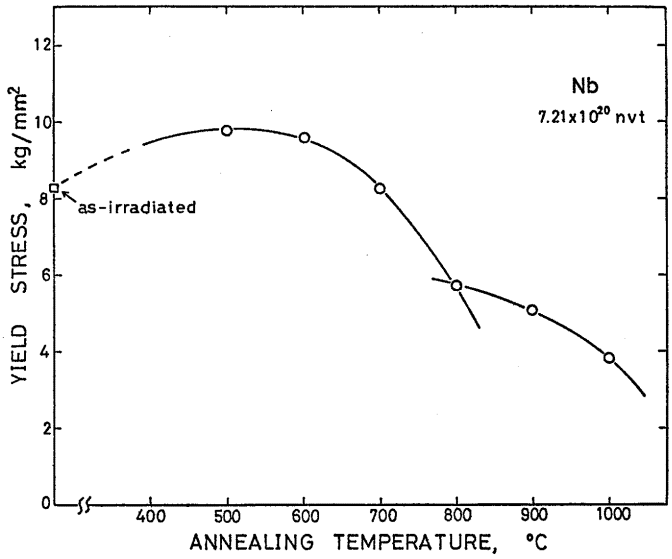

Fig. 7 Recovery process of the yield stress of neutron-irradiated niobium to a dose of 7.2×10^{20} n/cm. Each measurement was performed at room temperature.

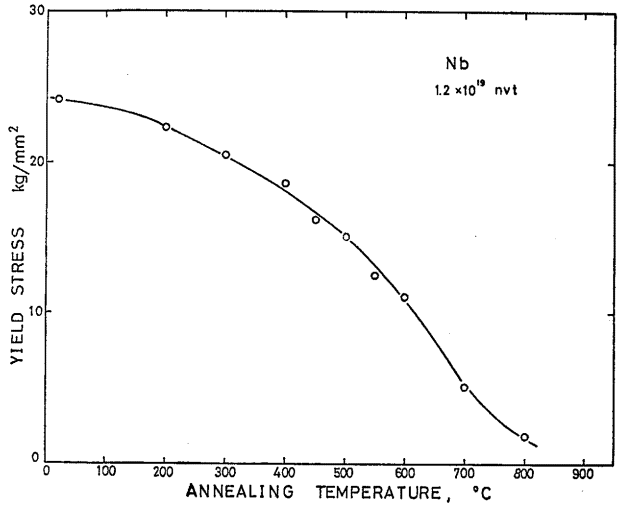

Fig. 8 Recovery process of the yield stress of niobium irradiated by neutron to a lower dose of 1.2×10^{19} n/cm². Each measurement was performed at room temperature.

1.2×10^{19} n/cm^2 showed a single stage recovery as shown in Fig. 8. In this case no microvoid can be expected to be formed, and only dislocation loops induced by irradiation cause hardening. The yield stress is very high because of the small grain size.

Transmission electron microscope observation was also performed for niobium foil irradiated under the same condition as the specimens for positron annihilation measurements. No visible void was observed, but dislocation loops and dislocations were observed. The density of dislocation loops in the specimens annealed at 700°C for 30 min was about 1.2×10^{14} cm^{-3} and the loop diameter was about 500Å. The dislocation density in the specimen annealed at 1000°C was about 1×10^{8} cm^{-2}. In the latter specimen dislocation loops were annealed out and but only dislocation lines were retained.

4. Discussions

It is well known that FWHM of the angular correlation curve decreases by introducing dislocations, vacancies, vacancy clusters and voids into crystal specimens. The amount of the decrement of FWHM depends upon the kind of the defects, and then it should be possible to identfy the defect from the angular correlation curve if only one kind of defect is present and the concentration is high enough to insure the saturation of positron trapping. Vacancies introduced by quenching or irradiation and dislocations introduced by deformation cause a narrowing of FWHM of 7 to 15 % in varous metals (Cu[17], Nb[18], Fe[19], and Mo[1,13]). It is known that depleted zones, vacancies of high density, introduced by neutron-irradiation give a rather larger narrowing (~20 %), e.g., in Fe[20] irradiated at 20°K and measured at 77°K. On the other hand, more than 25 % reduction in FWHM was observed in Mo[1], Al[10] and Ni[11] containing voids. It can be concluded from these results that the reducton in FWHM of niobium in the present experiments should be caused by voids introduced by neutron-irradiation. Electron microscope observations showed no voids in the specimens. It should be then concluded that irradiated niobium contains microvoids as small as could not be detected in the electron microscope (<30 Å). On the other hand, niobium-3wt%zirconium contains no microvoids but depleted zones which cause narrowing observed. Michel and Moteff[21,22] observed small voids in niobium but no void in niobium-1wt%zirconium irradiated by neutron at 425 °C. It can be deduced that the irradiation temperature in the present experiment (~300°C) is slightly lower than the threshold temperature for the visible void formation. Addition of zirconium to niobium suppresses the void formation because of the trapping of vacancies by zirconium atoms as suggested by Michel and Moteff[21].

Isochronal recovery experiments of yield strength of irradiated niobium showed two recovery steps, 750°C and 1000°C, in the case of higher dose irradiation, but only one step, 750°C or lower, in the case of lower dose

irradiation as mentioned above. It should be concluded that the lower temperature stage is attributed to annealing out of irradiation-induced dislocation loops and the higher one to that of microvoids. The increment of the yield stress due to dislocation loops[23] is given by $\Delta\tau=0.5\mu b(Nd)^{1/2}$, where N is the density of dislocation loop and d is the loop diameter, then $\Delta\tau$ was estimated as 1.3kg/mm^2, and$\sim$2.5 kg/mm^2 in total load, which is almost equal to the observed value in Fig. 7. On the other hand, using the relation for the void hardening[23], $\Delta\tau=\mu b(Nd)^{1/2}$, where N is the void density, d is the void diameter, the amount of microvoid hardening of about 2 kg/mm^2, which is obtained by subtracting the yield stress of unirradiated specimen, 3 kg/mm^2, from the total load, 5 kg/mm^2, gives the estimation for the microvoid density as 1.2×10^{15} cm^{-3} assuming d=30 Å. Microvoids of this density may have positron trapping power large enough to explain the marked reduction of FWHM, since it is equivalent to single vacancies of the concentration 2.4×10^{-6}, if positron trapping cross section of microvoid is assumed to be proportional to the geometrical cross section, and single vacancies of this concentration are able to trap positrons of the considerable percentage of the total number.

Acknowledgements

The authors wish to express their cordial thanks to Dr. K. Futagami and Mr. Y. Akashi for presenting us the informations of electron microscope observations in neutron-irradiated niobiums.

References

1) Mogensen, O, Petersen, K., Cotterill, R. M. J. and Hudson, B.: Effect of voids on angular correlation of positron annihilation photons in molybdenum, Nature **239** (1972) 98.
2) Petersen, K., Thrane, N. and Cotterill, R. M. J.: A positron annihilation study of the annealing of, and void formation in, neutron-irradiated molybdenum, Phil Mag. **29** (1974) 9.
3) Petersen, K., Knudsen, M. and Cotterill, R. M. J.: Changes in positron annihilation characteristics in molybdenum induced by neutron irradiation, Phil. Mag. **32** (1975) 417.
4) Thrane, N. and Evans, J. H.: The effect of impurities on the lifetime of positrons in voids in molybdenum, Appl. Phys. **12** (1977) 183.
5) Thrane, N. and Petersen, K. and Evans, J. H.: The relationship between void size and positron lifetime in neutron irradiated molybdenum, Appl. Phys. **12** (1977) 187.
6) Mackenzi, I. K. and Sen, P.: Correlation of positron age and pair momentum in radiation-induced voids in molybdenum, Phys. Rev. Lett. **37** (1976) 1296.
7) Hinode, K., Tanigawa, S., Doyama, M. and Shiraishi, K.: A study of the anneaing behavior of high-temperature neutron-irradiated molybdenum by means of positron lifetime, J. Nucl. Mat. **66** (1977) 212.

8) Triftshäuser, W., McGervey, J.D. and Hendricks, R.W. Positron annihilation studies of voids in neutron-irradiated aluminum single crystals, Phys. Rev. **B9** (1974) 3321.
9) Petersen, K. Thrane, N. and Trumpy, G.: Positron annihilation study of voids in a neutron irradiated aluminum single crystal, Appl. Phys. **10** (1976) 85.
10) Lindberg, V.W., McGervey, J.D., Hendricks, R.W. and Triftshäuser, W.: Annealing studies of voids in neutron-irradiated aluminium single crystals by positron annihilation, Phil. Mag. **36** (1977) 117.
11) Hasegawa, M. and Suzuki, T.: Positron annihilation in neutron-irradiated nickel single crystals, Radiation Effects **21** (1974) 201.
12) Nanao, S., Kuribayashi, K., Tanigawa, S, and Doyama, M.: Studies of voids in heavily neutron damaged nickel by positron annihilation, Mat. Sci. Eng. **18** (1975) 285.
13) Eldrup, M., Mogensen, O.E. and Evans, J.H.: A positron annihilation study of the annealing of electron irradiated molybdenum, J. Phys. **F6** (1976) 499.
14) Hautojärvi, P., Heinio, and Manninen, M. and Nieminen, R.: The effect of microvoid size on positron annihilation characteristics and residual resistivity in metals, Phil. Mag. **35** (1977) 973.
15) Jena, P., Gupta, A.K. and Singwi, K.S.: Positron annihilation in small metal voids, Solid State Comm. **21** (1977) 293.
16) Hasegawa, M., Suzuki, To. and Hirabayashi, M.: Angular correlation of photons from positron annihilation in copper-nickel alloys, J. Phys. Soc. Japan **37** (1974) 85.
17) Kuribayashi, K., Tanigawa, S., Nanao, S. and Doyama, M.: Phys. Lett. **40A** (1972) 27.
18) Dekhtyar, I. Ya, Mikhalenkov, V.S. and Sakharova, S.G.: Annihilation of positrons by electrons in plastically deformed metals having a bcc lattice, Soviet Physics-Doklady **11** (1966) 537.
19) Snead, C.L. Jr., Goland, A.N., Kusmiss, J.H., Huang, H.C. and Meade, R.: Influence of defects on the angular correlation of positron-annihilation photons in irradiated and in deformed iron, Phys. Rev. B **3** (1971) 275.
20) Weller, M., Triftshäuser, W. and Diehl, J.: Investigations of neutron irradiated iron by positron annihilation and internal friction measurements, 'Fundamental Aspects of Radiation Damage in Metals', Gatlinburg, Tennessee, USA (1975) 1136.
21) Michel, D.J. and Moteff, J.: Voids in neutron irradiated and annealed niobium and niobium-1% zirconium alloy, Radiation Effects **21** (1974) 235.
22) Jang, H. and Moteff, J.: The influence of neutron irradiation temperature on the void characteristics of niobium and niobium-1% zirconium alloy, Radiaton Effects and Tritium Technology for Fusion Reactors, Gatlinburg, Tennessee, USA (1975) I-106.
23) Moteff, J., Michel, D.J. and Sikka, V.K.: The infuence of irradiation temperature on the hardening behavior of the refractory bcc metals and alloys, 'Defects and Defect Clusters in B.C.C. Metals and Their Alloys', Gaithersburg, Maryland, USA (1973) 198.

(Received April 24, 1978)

Reports of Research Institute for Applied Mechanics
Vol. XXVI, No. 81, 1978

POSITRON LIFETIME MEASUREMENTS OF ELECTRON-IRRADIATED IRON AND IRON-CARBON

By Eiichi KURAMOTO* and Kazunori KITAJIMA**

Positron lifetime measurements have been performed in pure iron and iron-carbon irradiated by high energy electron (28 MeV) at 77°K. Measurements were performed at room temperature after each annealing at various temperatures above room temperature. Positron trapping by radiation-induced vacancies was observed, but disappeared mainly at single stage around 230°C in pure iron and at two stages around 100°C and 280°C in iron-carbon. The former should correspond to free migration of vacancies and the latter two correspond to migration and trapping of carbon atoms to vacancies and dissociation of carbon atoms from vacancies, respectively. Positron lifetimes were quite long (>300 psec) and could not be considered to correspond to monovacancies but small vacancy clusters. The value of lifetime increased with increasing annealing temperature in pure iron but remained constant in iron-carbon. The increase of lifetime means growth of vacancy clusters as observed in other metals, e.g., Mo and Cu.

1. Introduction

Although many investigations have so far been performed to obtain detailed knowledge of the properties of crystal defects in α-iron, very little has definitely been established. In particular, the views on migration energy of monovacancies, and on the interpretation of some of the recovery stages observed in α-iron have been quite controversial[1-7]. This is due partly to the extreme sensitivity of physical properties of defects in α-iron to the presence of interstitial impurity atoms, and partly to the presence of phase transformation between fcc γ-phase and bcc α-and δ-phases, which gives rise to additional difficulties for both quenching and high temperature equilibrium experiments.

Recently positron annihilation technique has become a powerful tool for the study of defects in crystals, particularly, vacancies, vacancy clusters and dislocations. Snead et al. measured the angular correlation of positron-annihilation photons in electron-irradiated iron and found the recovery stage

* Associate Professor, Research Institute for Applied Mechanics, Kyushu University.
** Professor, The Reseach Institute for Applied Mechanics, Kyushu University.

at 100°C, which is considered to be due to migration of carbon atoms to vacancy sites[8]. Weller et al. also obtained angular correlation curves in neutron-irradiated iron doped with carbon and concluded that migration stages of carbon atoms and vacancies were 50-100°C and 230-310°C, respectively, by comparing with the results obtained in internal friction measurements performed in parallel.[9] Schaefer et al. measured the Doppler broadening of the positron-annihilation line-shape for pure iron set in the cryostat where measurements in all temperature range were available and obtained informations of vacancies in thermal equilibrium.[10] They obtained the formation energy of vacancies 1.6 eV in α-iron and then 1.28 eV as migration energy of vacancies using the self-diffusion energy of 2.88 eV obtained in pure iron by tracer method.

In this report will be presented the results of positron lifetime measurements performed in electron-irradiated iron and iron doped with carbon. Positron lifetime depends on the size of vacancy clusters and then the informations on vacancy migration and clustering should be obtained from this measurement.

2. Experimental Procedures

2.1 Positron Annihilation Lifetime Measurements

For lifetime measurements one has to use positron sources which emit a fairly strong γ-radiation in coincidence with positrons, such as Na^{22} (see Fig . 1, where a lifetime of metastable Ne^{22} is very short, i.e., 3×10^{-13} sec and decays to a stable Ne^{22} with γ-radiation of 1.28 MeV). The coincidence radiation is used to trigger an 'electronic clock' at the time of birth of a positron. The essential component of the 'clock' is a time-to-amplitude

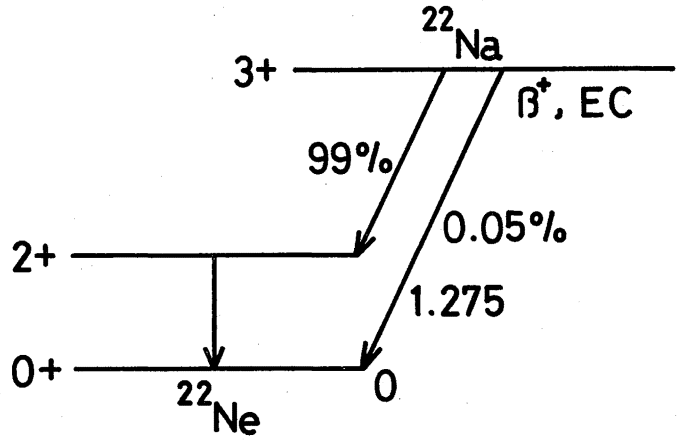

Fig. 1 Decay scheme of Na^{22} (positron source)

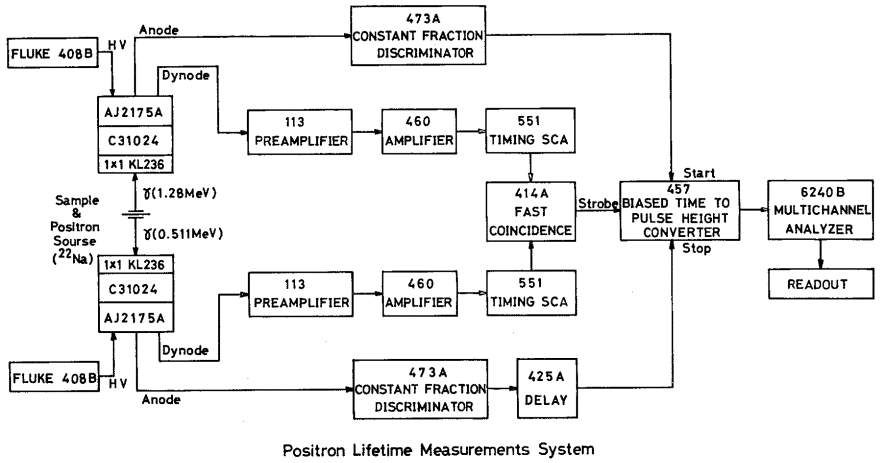

Fig. 2 Schematic diagram of the electronic circuit for positron annihilation lifetime measurement.

converter. The schematic diagram of electronic circuit is shown in Fig. 2. The time-to-amplitude converter generates an output whose amplitude varies linearly with the time between starting and stopping the clock. The 'stop' pulse is obtained from one of the γ rays of the annihilation radiation of the positrons. The output is stored in a multichannel analyser. The window for energy analysis in a timing single channel analyser (Timing SCA) is set as ± 10 % and the resolution time in a fast coincidence circuit is set as 20 nsec. If the lifetime τ to be measured is large compared with the width of the prompt resolution curve, the distribution of time intervals between starting and stopping the 'clock', and therefore of the pulse heights, is an exponential decay curve proportional to $\exp(-t/\tau)$. In practice the finite width of the time resolution function ($\sim$235 psec in FWHM in the present apparatus) causes a smearing of the decay function. The time resolution function was determined by measuring the pulse-height distribution from a source such as Co^{60} that emits two coincident γ rays.

Three component analysis has been performed for the obtained distribution of time intervals, namely, the shortest lifetime component τ_1, I_1 due to the annihilation in matrix, the second component τ_2, I_2 due to the annihilation at defects (mainly in vacancy or vacancy clusters) and the longest component τ_3, I_3 due to the annihilation in probaly positron source itself, $Na^{22}Cl(2\mu Ci)$ deposited on mylar thin plate. The analysis also contains the mylar component and the background. It took about 24 hours to measure $\sim$ 1,000,000 counts for one distribution curve and during the measurement the temperature must be kept constant within ± 1°C. Actual arrangement of a positron source and specimens is sketched in Fig. 3.

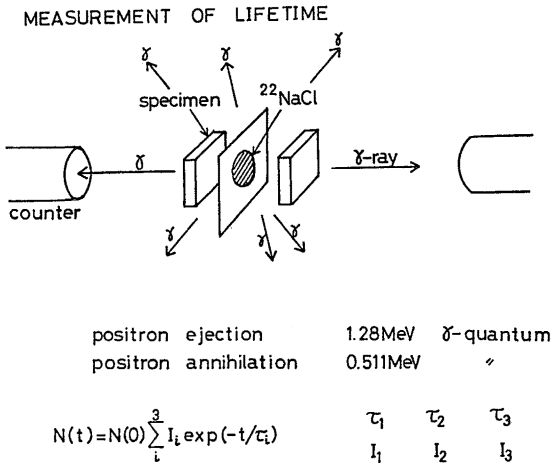

Fig. 3 Illustration of the arrangement of a positron source, specimens and probes.

2.2 Sample Preparation and Electron-Irradiation

High purity iron rod (MRC MARZ grade) was zone-refined in wet and dry hydrogen gas one and five times, respectively, then again zone-refined in vacuum (1×10^{-6} mmHg) two times. The zone-refined rod was then rolled into a thin sheet of 0.3 mm and annealed in wet and dry hydrogen gas at 880°C, 10 hr and 650°C, 1 hr, respectively. The residual resistivity ratio was 1300 at 300 Gauss (probably 2000 at 800 Gauss). Grain size was about 2 mm. Controlled amount of carbon atoms (100 wt. ppm) was doped into some of the specimens by annealing them in the hydrogen gas which had flowed through the liquid of n-hepthane. The doped specimen was then homogenized in argon gas and quenched into water to prevent carbon atoms from forming precipitations.

Electron-irradiation was performed using high energy accelerator (Kyoto University Research Reactor, LINAC, 28 MeV, 15 μA). Specimens were set in liquid nitrogen forced to flow in stainless steel channel which has a window of thin (0.05 mm) stainless steel plates from where electron beam comes in. The details of the apparatus was described in the previous paper[11].

3. Experimental Results

The results obtained on the lifetime τ_i and the respective intensity I_i of irradiated specimens and typical annihilation time spectra are given in Table I and Fig. 4, respectively. Unirradiated specimens also have non-vanishing I_2 components which might be due to grain boundaries. Electron-irradiation provides larger I_2 components which contain both contributions from radiation-induced point defects and grain boundaries. Annealing at each temperature

Table I

		τ_1 (psec)	τ_2 (psec)	τ_3 (nsec)	I_1 (%)	I_2 (%)	I_3 (%)
Fe[1]	unirr.	107	364	1.7	91.4	7.5	1.1
Fe[2]	unirr.	113	351	1.8	90.0	10.0	
Fe[1]	irr(50°C)	100	305	1.4	70.6	28.1	1.3
Fe[2]	irr(77°K)	108	361	1.8	81.8	18.2	
Fe[2]	100°C	109	369	1.9	83.2	16.8	
Fe[2]	170°C	113	383	1.9	84.5	15.5	1.2
Fe[2]	230°C	116	383	1.8	86.8	13.2	1.3
Fe[2]	270°C	117	388	1.8	89.2	10.8	1.3
Fe[1]	270°C	105	382	1.8	90.4	8.7	0.9
Fe[1]	330°C	104	369	1.6	92.5	6.7	0.8
Fe-C	unirr.	107	381		91.4	8.6	
Fe-C	irr(77°K)	107	311		62.5	37.5	
Fe-C	100°C	107	310		66.0	34.0	
Fe-C	170°C	107	335		77.6	22.4	
Fe-C	270°C	107	327		75.7	24.3	
Fe-C	300°C	103	336		87.5	12.5	

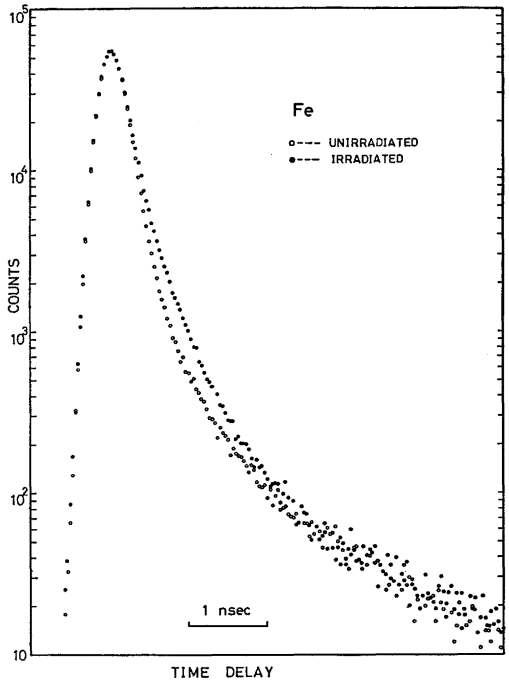

Fig. 4 Typical annihilation time spectra observed in pure iron unirradiated (open circles) and electron-irradiated (solid circles)

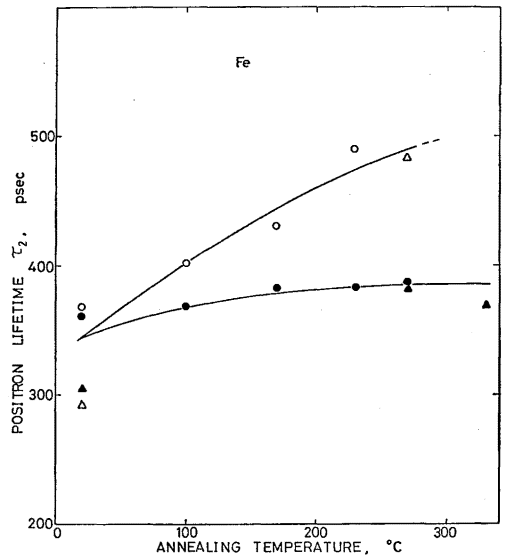

Fig. 5 Effect of isochronal annealing on τ_2 in pure iron electron-irradiated at 77°K (triangular points, at 40°C). Solid circles are experimentally obtained values and open ones are lifetimes for vacancies calculated from experimental data (see in text).

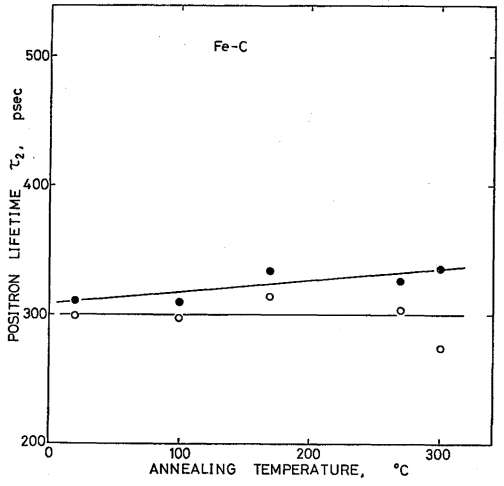

Fig. 6 Effect of isochronal annealing on τ_2 in iron-carbon electron-irradiated at 77°K. Solid circles are experimental data and open circles are lifetimes for vacancies calculated from experimental data (see in text).

(15 min, in vacuum of 5×10^{-7} mmHg) decreases I_2 component, which shows migration of radiation-induced defects (mainly vacancy type) to sinks occurs in this temperature range because grain boundaries should not show any recovery below 300°C. I_2 components of irradiated specimens were divided into two terms, (I_2^0, τ_2^0) and (I_2^1, τ_2^1). The former corresponds to the contribution from grain boundaries and the latter from radiation-induced defects (vacancies). These two terms were determined by simple calcula-

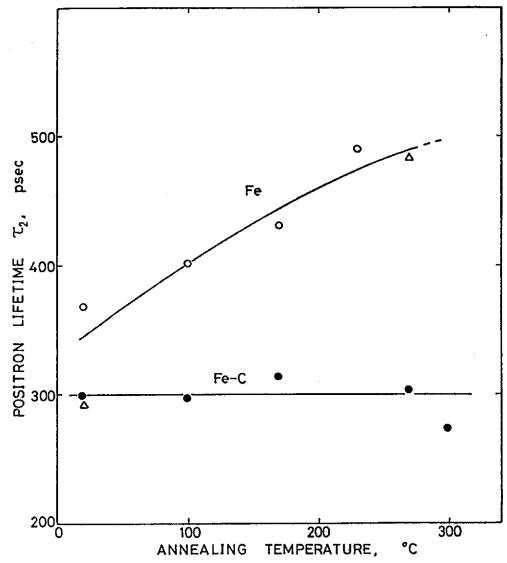

Fig. 7 Effect of isochronal annealing on τ_2 in electron-irradiated pure iron and iron-carbon (replotted from Figs. 4 and 5),

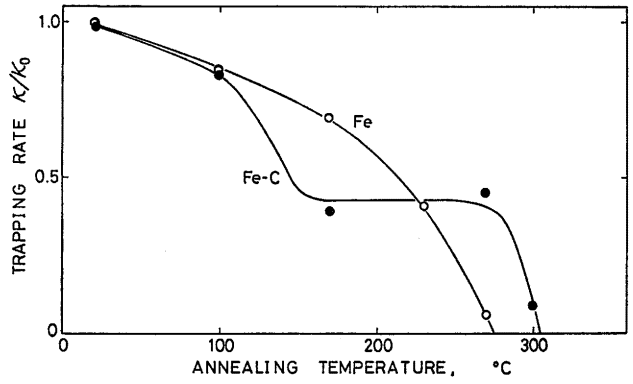

Fig. 8 Effect of isochronal annealing on κ in electron-irradiated pure iron and iron-carbon

tions using trapping model (described below) and comparing I_2 components of unirradiated and irradiated specimens. Results are shown in Figs. 5 and 6, wher evalues of τ_2 (solid circle) and τ_2^1 (open circle) are plotted against annealing temperature in the case of pure iron and iron-carbon, respectively. In Fig. 7 values of τ_2 for the radiation-induced defects, τ_2^1, are replotted against annealing temperature. As shown in this figure τ_2 in pure iron increases with increasing annealing temperature, but that in iron-carbon remains constant. In Fig. 8 trapping rates of positrons to radiation-induced defects (vacancy or vacancy clusters) are plotted against annealing temperature. These values were calculated together with values of τ showed above. Details of the method of the calculations and trapping model of positrons will be described below.

If only one kind of defects trap positrons in specimens, the time change of the number of untrapped (free) positrons, N_f, and that of trapped positrons, N_t, are given by

$$\begin{aligned}\frac{dN_f}{dt}&=-\lambda_1 N_f-\kappa N_f\\ \frac{dN_t}{dt}&=-\mu_2 N_t+\kappa N_f\end{aligned} \tag{3.1}$$

with the solutions

$$N(t)=N_f(t)+N_t(t)=N(0)[I_1\exp(-\mu_1 t)+I_2\exp(-\mu_2 t)] \tag{3.2}$$

where $\mu_1=\tau_1^{-1}=\lambda_1+\kappa$, $\mu_2=\tau_2^{-1}$, $I_1=1-\kappa(\mu_1-\mu_2)^{-1}$, $I_2=\kappa(\mu_1-\mu_2)^{-1}$, λ_1^{-1} is the lifetime of free positrons, τ_2 is that of trapped positrons, κ is the trapping rate of positrons to defects. If there are two kinds of defects which trap positrons, e.g., vacancies and grain boundaries like the present experiments, the solution is likewise given by

$$N(t)=N(0)[I_1\exp(-\mu_1 t)+I_2\exp(-\mu_2 t)+I_2'\exp(-\mu_2' t)] \tag{3.3}$$

where $\mu_1=\tau_1^{-1}=\lambda_1+\kappa+\kappa'$, $\mu_2=\tau_2^{-1}$, $\mu'_2=\tau'^{-1}_2$, $I_1=1-\kappa(\mu_1-\mu_2)^{-1}-\kappa'(\mu_1-\mu_2')^{-1}$, $I_2=\kappa(\mu_1-\mu_2)^{-1}$, $I_2'=\kappa'(\mu_1-\mu_2')^{-1}$, τ_2, τ'_2 and κ, κ' are positron lifetimes and trapping rates for two kinds of defects, respectively. The second components (τ_2 and I_2) of irradiated specimens in Table I contain two contributions from two kinds of trapping centers, grain boundaries and vacancies and the next relation is approximately established, denoting experimentally obtained values as I_2^e and μ_2^e.

$$I_2^e\exp(-\mu_2^e t)=I_2\exp(-\mu_2 t)+I'_2\exp(-\mu'_2 t) \tag{3.4}$$

The two cases, $t=0$ and $t\simeq 0$ give two relations as follows.

$$\begin{aligned}I_2^e&=I_2+I'_2\\ I_2^e\mu_2^e&=I_2\mu_2+I'_2\mu'_2\end{aligned} \tag{3.5}$$

Using the values of τ_2 and κ of unirradiated specimens we can solve this set of equations, givng the values of τ_2 and κ for radiation-induced vacancies which were already shown in Figs. 5, 6, 7 and 8.

4. Discussions

Most of the expriments so far performed show that vacancy migration in iron occurs above room temperature, but very few show the migraton below room temperature, e. g., Cuddy[12] and Doyama et al[13]. Our measurements were performed only above room temperature, so that informations between 77°K and room temperature were not obtained. Table I, however, shows the dominant migration of vacancies occurs about 230°C in pure iron, although Fig. 7 shows the gradual increase of τ_2, which means clustering of vacancies according to Hautojärvi et al[14], already started at room temperature as shown in Fig. 7. In the interpretation of the experimental results it must be taken into account that the energy of electrons used for irradiaton was so high as 28 MeV that collision produces multiple displacements and then the distribution of radiation-induced defects is not necessarily uniform, i. e. some parts of them must be localized foming concentrated regions like depleted zones in neutron-irradiation. In that case clustering of vacancies is expected to occur at lower temperatures because the distance to the neighbouring vacancies is very short (a few atomic distances) compared with that in uniform distribution. This might be one of the causes lowering the temperature for vacancy migration in the present experiments. In Doyama et al's case (neutron-irradiated iron), this effect must be much more prominent, which can be regarded as the main reason lowering the migration temperature (~200°K).

The other problem is that the value of τ_2 itself is already larger than 300 psec at room temperature in pure iron. It is known that in various metals positron lifetime in single vacancies and that at dislocations are almost equal each other. In iron positron lifetime at dislocations was measured as 167 psec by Hautojärvi et al[15] using deformed iron specimens. Positron lifetime in single vacancies in iron may then be less than 200 psec in the analogy of other metals though it has not yet been measured. The value of τ_2, 300 psec is, therefore, may not be a positron lifetime for a single vacancy, but that for a small vacancy cluster, probably, di-or tri-vacancy according to Hautojärvi et al's calculation[14]. It must be hence concluded that clustering of vacancies already occured below room temperature, presumably, in vacancy concentrated regions in the specimen, where a few atomic distance jump of vacancies form small clusters.

Recently kiritani et al[16] obtained the vacancy migration stage 310°C~340°C in pure iron by the observation of interstitial-type dislocation loop formation in high voltage electron microscope. But it was not confirmed whether the migration process corresponds to single vacancies or other clus-

ters. If we assume the migration stage of single vacancies in iron is below room temperature, e.g. ≃200°K (~0.6 eV), the formation energy should be 2.28 eV because the self-diffusion energy has been established as 2.88 eV from the experiment using a radio-tracer method[17]. The formation energy 2.28 eV is, however, too large to dope enough vacancies for electrical resistivity measurements to specimens by quenching from 900°C. On the other hand, Takaki and Kimura[6] succeeded in observing the vacancy migration stage on the resistivity recovery curve of quenched specimen. Hence it seems reasonable to think that vacancy migration stage exists above room temperature except the case where highly vacancy-concentrated region, e.g., depleted zone in neutron-irradiation, can be expected to exist.

In iron doped with carbon τ_2 did not increase but remained constant as ~300 psec and trapping rate κ decreased stepwisely, namely, ~100°C and 280°C as shown in Figs. 7 and 8, respectively. The first stage must correspond to migration of carbon atoms to vacancy sites, giving rise to the reduction of trapping cross section for positrons, i.e., decrease of trapping rate κ. This is the same result as those of angular correlation experiments performed in iron doped with carbon irradiated by electrons (Snead et al[8]) and neutrons (Weller et al[9]). Constancy of τ_2 in iron-carbon for isochronal annealing could be explained by this complex formation (probably a carbon atom plus di-or tri-vacancies). The stable configuration of complex of a carbon atom and a single vacancy was calculated by Johnson[18], where a carbon atom stays just beside the vacancy site and did not go into the vacancy. The stable configuration of complex of a carbon atom and di-or tri-vacancy has not yet been calculated, but presumably, a carbon atom goes into the vacant sites to decrease the trapping power for positrons. The second stage, ~280°C, can be considered as dissociation of the complex and vacancies rapidly migrate to sinks, causing the decrease of trapping rate κ.

Acknowledgements

The authors wish to express their cordial thanks to Dr. T. Chiba and Dr. N. Tsuda in National Institute for Researches in Inorganic Materials for main parts of positron annihilation lifetime measurements and presenting many suggestions in technical problems of lifetime measuring electronic circuit. A part of this work was done under the Visiting Researchers Program of Kyoto University Research Reactor Institute. The authors also express their thanks to Dr. H. Yoshida in KURRI.

References

1) Fujita, F.E. and Damask, A.C.: Kinetics of carbon precipitation in irradiated iron-II, Electrical resistivity measurements, Acta Met. **12** (1964) 1215.
2) Glaeser, W. and Wever, H.: Quenching experiments with high purity iron, Phys. Stat. Sol. **35** (1969) 367.

3) Ichikawa, F., Yamakawa, K. and Fujita, F. E. : Lattice defects in quenched high purity iron, Scripta Met, **6** (1972) 929.
4) Wever, H. and Seith, W. : Quenching experiments with high purity iron, Phys. Stat. Sol. (a) **28** (1975) 187.
5) Ikeda, Y., Gotoh, T., Abiko, K. and Kimura, H. : An estimate of vacancy migration energy from aging experiments in an iron 3.8 at% molybdenum alloy, Crystal Lattice Defects **5** (1974) 163.
6) Takai, S. and Kimura, H. : Preparation of high-purity iron by electron-beam floating-zone melting under ultra-high vacum, Scripta Met. **10** (1976) 1095.
7) Diehl, J., Merbold, U. and Weller, M. : Information on vacancy migration in α-iron from annealing experiments, Scripta Met. **11** (1977) 811.
8) Snead, C. L. Jr., Goland, A. N., Kusmiss, J. H., Huang, H. C. and Meade. R. : Influence of defects on the angular correlation of positron-annihilation photons in irradiated and in deformed iron, Phys. Rev. B **3** (1971) 275.
9) Weller, M., Trifthäuser, W. and Diehl, J. : Investigations of neutron irradiated iron by positron annihilation and internal friction measurements, 'Fundamental Aspects of Radiation Damage in Metals', Gatlinburg, Tennessee, USA (1975) 1136.
10) Schaefer, H. E., Maier, K., Weller, M., Herlach, D., Seeger, A. and Diehl, J. : Vacancy formation in iron investigated by positron annihilation in thermal equilibrium, Scripta Met. **11** (1977) 803.
11) Kitajima, K., Futagami, K., Kuramoto, E., Abe, H., Tsukuda, N., Akashi, Y., Yoshida, H. and Fujita, A. : Application of KUR LINAC to the study of radiation damage in metals, Annual Reports of the Research Peactor Institute, Kyoto University **10** (1977) 91.
12) Cuddy, L. J. : Recovery of point defects in iron after low temperature deformation, Acta Met. **16** (1968) 23.
13) Doyama, M. : Private commumication.
14) Hautojärvi, P., Heinio, J., Manninen, M. and Nieminen, R. : The effect of microvoid size on positron annihilation characteristics and residual resistivity in metals, Phil. Mag. **35** (1977) 973.
15) Hautojärvi, P., Vehanen, A. and. Mikhalenkov, V. S. : On interactions of dislocations and impurities in deformed iron and copper, Fourth International Conference on Positron Annihilation, Helsingor, Denmark, (1976).
16) Yoshida, N., Kiritani, M. and Fujita, F. E. : Electron radiation damage of iron in high voltage electron microscope, J. Phys. Sol. Japan **39** (1975) 170.
17) Hettich, G., Mehrer, H. and Maier, K. : Self-diffusion in ferromagnetic α-iron, Scripta Met. **11** (1977) 795.
18) Johnson, R. A., Dienes, G. J. and Damask, A. C. : Calculations of the energy and migration characteristics of carbon and nitrogen in alpha iron and vanadium, Acta Met. **12** (1964) 1215.

(Received April 24, 1978)